Dark Matter in a Single-metric Universe

C.C. Wong
Department of Electrical and Electronic Engineering, University of Hong Kong. H.K.
E-mail: ccwong@eee.hku.hk

Abstract

Cosmological models connecting the static Schwarzschild metric with the time dependent Friedmann-Robsertson-Walker (FRW) metric [1-2] generally support only zero-pressure continuity at some interface. Instead of matching two different metrics at an interface, Baker [1] proposed the use of the Lemaître-Tolman metric which can go smoothly from a Schwarzschild-Lemaître metric near a mass concentration to the Friedmann-Lemaître metric at large distances and also allows for non-zero pressure. Using a variant of the Bona-Stela condition, we fix a metric and find that the geodesic equation contains in its slow-speed limit an effective dark matter (eDM) term. We show that this eDM can explain the effects of the dark matter such as the flatten rotational curve of galaxies, the desirable growth rate for the baryonic matter density perturbation during the matter dominant epoch and the dark matter enhancement on the higher acoustic peaks of the power spectrum of the CMB anisotropies.

1 Introduction

The Planck estimate [3] of visible matter, dark matter and dark energy densities for our present epoch provides an appealing description of the energy density components of the universe. However the nature of dark matter and dark energy remain unresolved. So far dark matter particles have not been found within our solar system [4]. Alternative ideas are investigated to explain dark matter involving modified gravity theories such as Conformal Gravity and MOND, see for example [5-9]. MOND is an interesting phenomenological theory which is successful at galactic distances but becomes problematic at larger distances and at early epochs. One challenge is to understand the MOND effects in a more fundamentally motivated relativistic

frame-work which could account for the effects of dark matter where MOND is problematic. Most cosmological models connecting the FRW spacetime with the Schwarzschild metric [1-2] are constructed by matching densities and pressures from both metrics with continuity at the interface. The pressure is generally taken to be zero due to the static Schwarzschild metric. To accommodate varying background pressure from radiation dominant to dark energy dominant epoch, Baker [1] proposes to use a single Lemaître-Tolman metric which approaches asymptotically to the Schwarzschild-Lemaître metric at small distances while asymptotically approaches to the Friedmann-Lemaître metric at large distances. For a flat universe, we use a variant of the Bona-Stela condition in [1] to specify the metric. In the slow speed limit, we find that the equation of motion possesses an additional "effective dark matter" eDM term. This eDM becomes significant when the background energy density is comparable to the mass density of the spherical symmetric system. In a spiral galaxy, at large distances near a cut-off distance the eDM becomes dominant and behaves like a massive halo and predicts a flatten rotational curve. Using the estimates of the Milky Way, at smaller distances near a minimum potential "bulge", the eDM density is negligible comparing to visible mass density and the orbits are Newtonian. The effect of the eDM from the bulge to the cut-off distance is to provide a much steeper non-Newtonian potential that prevents matter from following the Keplerian orbits. Matter will follow a shorter spiral path to accrete around Newtonian dominant orbits. For the rotational curve observations in the Milky Way, based on a single higher mass to luminosity ratio around the bulge the rotational curve matches the observations extremely well up to 100 kpc. This eDM term also predicts a non-Newtonian flatten rotational curve from 300 kpc up to the galactic cutoff. The total mass is estimated to be around 3 times the observable mass. During the early matter dominant epoch, with the presence of the eDM the baryonic matter perturbation growth rate is driven by the eDM and and grows as the square of its no-eDM rate and is thus fast enough to reach unity at low redshift and provides a natural mechanism for the large scale structure growth and Early Reionization. We also discuss how the eDM can lift the higher peaks observed in the CMB power spectrum. Where appropriate we comment on the eDM's effect on the dynamical mass increase in clusters of galaxies and the suppression of the Baryon Acoustic Oscillations.

2 The model

In order to investigate the effects of expansion on locally bound systems like galaxies, one looks at the geodesics of test particles in the appropriate metric that describes the spacetime in the vicinity of a point mass M placed in an expanding cosmological background. One would need to find a metric which reproduces a time dependent FRW metric at large distance and a spherical symmetric metric at small distances, which can also accommodate non-zero pressure. Here we highlight the essential steps of the work of [1] where the metric is given by the Lemaître-Tolman formalism

$$ds^2 = -e^{2\alpha(\varrho,t)}d\varrho^2 - e^{2\beta(\varrho,t)}d\Omega^2 + c^2dt^2 \tag{2.1}$$

$$d\Omega^2 = d\theta^2 + sin^2\theta d\varphi^2 \tag{2.2}$$

where c is the speed of light, t is the proper time, ϱ is the comoving distance. The choice of $\alpha(\varrho,t)$ and $\beta(\varrho,t)$ has to approach asymptotically to FRW metric at large distance and a spherical symmetric metric at small distance. Assuming spatial curvature is isotropic, $\theta = \frac{\pi}{2}$ and space is "flat", in our time-orthogonal system α can be chosen to be

$$e^{\alpha} = \frac{\partial\beta}{\partial\varrho}e^{\beta}, \tag{2.3}$$

Different solutions of β represents different metrics. For example, $e^{\beta} = a(t)\varrho$, $e^{\alpha} = a(t)$, $a(t)$ being the scale factor, gives the Friedmann- Lemaître metric, while $e^{\beta} = R$, $e^{2\alpha} = r_s/R$, where R the proper distance and r_s the Schwarzschild radius are defined in the usual way, leads to the Schwarzschild-Lemaître metric. The equation of motion depends solely on the choice of $\beta(\varrho,t)$. We use a variant of the Bona-Stela choice:

$$8\pi T_1^1 = 2\frac{\ddot{\beta}}{c^2} + 3(\frac{\dot{\beta}}{c})^2 - \Lambda = 2\frac{\ddot{a}}{ac^2} + 3(\frac{\dot{a}}{ac})^2 + \frac{4}{3c^2}(3-\eta)\frac{\dot{a}}{a}\frac{C_2\dot{\omega}}{(C_1+C_2\omega)} - \Lambda, \tag{2.4}$$

where T_{ν}^{μ} is the stress momentum tensor and Λ is the cosmological constant. β is then given by the general solution

$$e^{\beta(\varrho,t)} = a(t)[C_1(\varrho) + C_2(\varrho)\omega(t)]^{2/3}, \ where \ \omega(t) = \int_{t_0}^{t}\frac{d\tau}{a(\tau)^{\eta}}. \tag{2.5}$$

where $C_1(\varrho)$, $C_2(\varrho)$ are arbitrary function of ϱ. The choice $\eta = 3$ is the original Bona-Stela choice. We also have

$$8\pi T_4^4 = 3\dot{\beta}(\frac{\dot{a}}{a} + \frac{2}{3}\frac{C_2'\dot{\omega}}{(C_1' + C_2'\omega)}) \tag{2.6}$$

where an overdot means differentiation with respect to t. For the choice $\eta = 3/2$

$$\dot{\beta} = \frac{\dot{a}}{a} + \frac{2}{3}\frac{C_2\dot{\omega}}{(C_1 + C_2\omega)} = \frac{\dot{a}}{a} + \frac{2}{3}\frac{C_2}{r^{3/2}}, \tag{2.7}$$

for C_2 small and ϱ large, T_1^1 will go to the FRW solution, so that in this case that $\eta = 3/2$ is the only choice that the second term in $\dot{\beta}$ does not have $a(t)$ dependence. The Newtonian (slow speed) limit of the equations of motion of a point mass at a proper distance r is given in detail by

$$\ddot{r} = \frac{\ddot{a}}{a}r - \frac{2C_2(\varrho)^2}{9r^2} + \frac{1}{3}\frac{\dot{a}}{a}\frac{C_2(\varrho)}{r^{3/2}}r + \frac{c^2C_0^2}{r^3} - \frac{2C_0^2c^2C_2^2}{3r^4}, \tag{2.8}$$

where $C_1(\varrho) = C_2(\varrho)\varrho/c$ is chosen so that the $8\pi T_4^4$ goes to $3(\dot{a}/a)^2$ for large ϱ and provides the right relativistic correction to Newton's law as we shall see. We take $c^2C_0^2 = h^2$, where h is generally identified with constant angular momentum per unit mass of the system. In order to match the Newton's result, we follow Baker's choice

$$C_2(\varrho) = -\frac{3}{2}\sqrt{2GM}, \tag{2.9}$$

here the negative sign is chosen to preserve the Schwarzschild-Lemaître singularity at $\varrho = c\omega(t)$ and M is the mass of the system at the centre of the spherical symmetric metric. The model leads to the result

$$\ddot{r} = \frac{\ddot{a}}{a}r - \frac{GM}{r^2} - \frac{\dot{a}}{a}\sqrt{\frac{GM}{2r}} + \frac{h^2}{r^3} - \frac{3GMh^2}{c^2r^4}, \tag{2.10}$$

where the r^{-4} term is the relativistic correction and $h^2 = v^2r^2 = GMr$ is used in this term. We note that $\frac{\dot{a}}{a} = H$ is the Hubble parameter governed by the Friedmann equations

$$(\frac{\dot{a}}{a})^2 = H^2 = \frac{8\pi G}{3}\rho + \frac{\Lambda}{3} \tag{2.11}$$

where ρ is mass density of the background universe. The present value H_0 is given by [4].

$$\frac{\dot{a}}{a} \sim H_0 = 2.4 \times 10^{-18}s^{-1}. \tag{2.12}$$

We note that this relatively small value of H_0 introduces a scale below which the Newtonian acceleration dominates and a cutoff scale above which the

FRW acceleration dominates. The potential that produces the acceleration in Eq. (2.10) is given by (leaving out the relativistic correction term)

$$V(r) = \frac{h^2}{2r^2} - \frac{GM}{r} + H\sqrt{2GMr}. \tag{2.13}$$

In the following sections we explore whether this eDM term can provide a consistent description for dark matter in various situations.

3 The Tully-Fisher relation, the matter spirals and the galaxy cut-off size

Using Eq.(2.10), we study the rotational speed of galactic dust in galaxies. At the galactic distance scale we make a first approximation by neglecting the constant angular momentum and the relativistic correction we find that,

$$v^2 = [\frac{GM}{r^3} + \sqrt{\frac{GM}{2r^3}}H - \frac{\ddot{a}}{a}]r^2 \tag{3.1}$$

where v is the rotational speed of galactic dust and M is the luminuos galactic mass. The empircal Baryonic Tully-Fisher relation (TFR) is given by

$$v^n \propto M; \;\; for \;\; n = 3.5 \sim 4 \tag{3.2}$$

From Eq.(3.1) one sees that at short distances when mass density is large, the rotational speed is described by Newtionian laws. When the Newtonian with non-Newtonian mass densities combined is much smaller than the $\ddot{a}/a$ term the attractive forces cease, there is no rotation but just acceleration away from centre of mass. It is when visible mass density $\rho(r)$ approaches the point where $H^2 \sim 2GM/r^3 \sim \frac{8\pi G}{3}\rho(r)$ the eDM term becomes significant and this term leads to

$$v^4 \approx \frac{1}{2}GMH^2r \tag{3.3}$$

written in the Tully-Fisher form. For general spiral galaxies, v^4 has an asymptotic limit at the Hubble radius $r_H = \frac{c}{H_0}$ where c is the speed of light

$$v^4 \approx \frac{1}{2}GMcH_0. \tag{3.4}$$

Here the acceleration, the gradient of the TRF is $3.6\times10^{-10}m/s^2$ in Eq.(3.4) which differs by a factor of 3 from the MOND acceleration $a_0 \approx 1.2 \times 10^{-10}m/s^2$ in the MOND formula $v^4 \approx GMa_0$. The similarity in order

of magnitude of the a_0 and cH_0 is a long-time puzzle raised by MOND proponent, see [5]. We note that Eq.(3.4) only provides a large distance TFR when the galaxy has a large cut-off size. The situation is more elaborated for a smaller cut-off size as discussed below. Guided by the dimensional analysis of the TFR, apart from the eDM one could also obtain solution such as

$$V(r) = br + c \tag{3.5}$$

where V(r) is an additional potential to the Newtonian potential and b and c are fine-tuning constants. This potential is a key feature of the Conformal Gravity program [9], in which the linear potential arises from the effects of the matter and curvature of galaxy's cosmological background. The discussions with the Conformal Gravity program can be found in [5]. We would like to point out that apart from the difference in algebraic form in r, our solution has no free parameter, has a built-in cosmological factor H which will vary according to the dominant energy density at the background and there is no modification of the Einstein Gravity.

To estimate the size of the cut-off distance of Milky Way, the simplest way is assuming that the halo is within a spherical shell. Take our current galactic mass estimate $\approx 3 \times 10^{42}$ kg. We write Eq. (3.1) in terms of the deceleration parameter q, which is negative in the acceleration epoch by

$$\frac{\ddot{a}}{a} = -qH^2 \tag{3.6}$$

We estimate the cutoff value of r by solving Eq.(3.1) at $v^2 = 0$ one obtains

$$R^3_{cutoff} = \frac{8GM}{H^2(\sqrt{1-8q}-1))^2} \tag{3.7}$$

We note that in the matter dominant epoch where q is positive, there is no cut-off radius. We introduce $H_0^2\Omega_{i,0} = \frac{8\pi G}{3}\rho_{i,0}$ where i denotes various energy density components with the normalisation constraint for spatially flat metric,

$$\Omega_{b,0} + \Omega_{eDM,0} + \Omega_{\Lambda,0} = 1 \tag{3.8}$$

From more empirical estimates, the deceleration parameter at the present epoch is given by $q(z \geq 0.09) = -0.34 \sim -0.38$ [Ref.10, Table II] whereas we have

$$q_0 = -\Omega_\Lambda + \frac{1}{2}(\Omega_b + \Omega_{DM}) \approx -0.524 \tag{3.9}$$

based on the ΛCDM Planck estimate. To be model independent for now, we take the empirical values for now $q(z \geq 0.09) \approx -0.34 \sim -0.38$, the cut-off radius becomes respectively

$$R_{cutoff} = 6.45 \sim 6.85 \times 10^{22} m \sim 2Mpc \tag{3.10}$$

where the observed general spiral galaxy halo radius is of order $10^{22}m$ [11]. This cut-off halo size will shrink as q decreases.

To see how the eDM affects the motions in a spiral galaxy such as the Milky Way, we note that from the Bertrand Theorem that for attractive forces only an inverse square law can produce a stable closed non-circular orbit. The eDM term is therefore more likely to produce unclosed orbit. To see this, we note that for a particle (dust) mass m and angular momentum $L = hm$ under the influence of a central potential with polar coordinate (r, φ) see for example [12], its orbital path is given by the equation,

$$\varphi - \varphi_0 = \int_{r_0}^{r} \frac{r^{-1} dr}{\sqrt{\frac{2}{h^2}(E/m - V)r^2 - 1}} \tag{3.11}$$

where E is the total energy and V is the Newtonian plus the eDM potential obtained from Eq. (2.13). From the minimum of the potential V, we note that the equilibrium distance between the angular momentum and the Newtonian potential is $r_{eq} = h^2/GM$, which is essentially the same as that of the full potential including the eDM potential since the eDM effective distance $r \sim (2GM/H^2)^{1/3}$ is far from r_{eq}. Eq.(3.11) becomes

$$\varphi - \varphi_0 = \int_{r_0}^{r} \frac{r^{-1} dr}{\sqrt{\frac{2}{h^2}(k/r + E/m - H_0\sqrt{2kr})r^2 - 1}}; \tag{3.12}$$

where $k = GM$. We follow the parametrisations in [12] by taking an appropriate length scale l with $h^2/(2k) = l$, and $r/l = \bar{\rho}$ and $y^2 = 1/\bar{\rho}$,

$$\varphi - \varphi_0 = -2 \int_{\frac{1}{\sqrt{2}}}^{y} \frac{dy}{\sqrt{1 - y^2 + E_0 y^{-2} - \lambda y^{-3}}}, \tag{3.13}$$

where $E_0 = (El)/(mk)$ and $\lambda = H_0\sqrt{2l^3/k}$ and we integrate only from distances larger than r_{eq}. We note that in Eq.(3.12, 3.13) that for $\lambda = 0$, $l = r_{eq}/2$ the orbits are the Keplerian. For non-zero λ, $r_{eq} = 2l$ becomes the largest scale where orbit remains Newtonian. For example in the Milky Way, the eDM potential term satisfies $H_0\sqrt{2/k}r^{3/2} < 1$ upto $\bar{\rho} = r/l \sim 200$

where the integrand in Eq. (3.12) is well defined, so that the eDM potential term can be treated as small for distances up to $\bar{\rho} \sim 200$. In the following we assume that we are dealing with spiral galaxies similar to the Milky Way. To understand the Eq.(3.13) we see that it is hard to solve exactly, but we know we have the Keplerian solution for small λ, so we make an expansion around small λ for the simplest case $E_0 = 0$,

$$\varphi - \varphi_0 \approx -2 \int_{\frac{1}{\sqrt{2}}}^{y} \frac{dy}{\sqrt{1-y^2}} - \int_{\frac{1}{\sqrt{2}}}^{y} \frac{\lambda dy}{y^3(1-y^2)^{3/2}} \tag{3.14}$$

both integrals in Eq.(3.14) can be intergrated, for large $\bar{\rho}$

$$\varphi - \varphi_0 = sin^{-1}(1 - 2/\bar{\rho}) + \frac{1}{2}\lambda\bar{\rho} + \lambda\frac{3}{4}\ln\bar{\rho} \tag{3.15}$$

Here for $\bar{\rho} \sim 200$ we have $1/\sqrt{\bar{\rho}}$ small, and $\lambda\bar{\rho}^{2/3} = \lambda_0 < 1$ nearly constant,

$$\varphi - \varphi_0 = \frac{\pi}{2} - \frac{2}{\sqrt{\bar{\rho}}} + \frac{1}{2}\frac{\lambda_0}{\sqrt{\bar{\rho}}} \tag{3.16}$$

Neglecting the phase angle, we have

$$\varphi = -\frac{2 - \lambda_0/2}{\sqrt{\bar{\rho}}} = -\frac{(2 - \lambda_0/2)\sqrt{l}}{\sqrt{r}} \tag{3.17}$$

which describes a hyperbolic spiral with narrower angular change from the Keplerian orbit for a large range of r near the cut-off scale. For $\bar{\rho} \sim 2$ and $r \sim r_{eq}$ the λ term in Eq. (3.14) approaches a constant$\times\lambda$ and can be absorbed into φ_0, and also we have $\lambda\bar{\rho}^{2/3} \ll 1$ in Eq.(3.12), one obtains for $\varphi_0 = \pi/2$ a Keplerian orbit

$$\bar{\rho} = \frac{2}{(1 - \epsilon cos\varphi)}; \quad r = \frac{r_{eq}}{(1 - \epsilon cos\varphi)} \tag{3.18}$$

where $\epsilon = \sqrt{1 + 4E_0}$ is the eccentricity of the Keplerian orbit. Starting from large $\bar{\rho}$ (and thus large r) at $\lambda = 0$ we recover an elliptic ($E < 0$) or parabolic ($E = 0$) path with the closest point to centre at $\bar{\rho} = 2$, or $r = r_{eq}$. For non-zero λ, Eq.(3.17) implies that for large $\bar{\rho}$ the dust will take a spiral path to move toward the centre of mass until $\lambda\bar{\rho}^{3/2}$ becomes small that Eq.(3.18) takes over and the dust will move in a Newtonian orbit. One effect of eDM is therefore to cause the baryonic matter from the large-distance halo region to follow a non-Keplerian spiral orbit into the rim of the Newtonian dominant region $r = r_{eq}$ so that here the matter density is of unusally high value due

to matter accumulations.

To see the impact this eDM term have on the rotational speeds, we use the data from [Ref. 13 table 2] for our Milky Way and Eq. (3.1) to plot the rotational speed of dust [see Figure 1a-1b]. We observe that a first flattening of rotational speeds occurs around $9 \sim 30$ kpc but the speeds start to fall off as distance grows. Phenomenologically one can choose a fixed dotted line around the first flattening range, which is a crudest MOND estimate depending on some galactic mass estimate. (Realistic MOND theories include an interpolating function between Newtonian acceleration and the MOND acceleration.) Alternatively the observations can be explained by a higher accumulation of matter at Newtonian orbits around 16 kpc where the eDM term is insignificant. This is where the central bulge, consisting mainly of old stars of lower luminosity to mass ratio, is located, and that these old stars provides evidence supporting a history of the accretions towards the bulge from larger distances as suggested by the eDM term. The derived mass limit in Ref.13 is 2×10^{42} kg upto 200 kpc. We assume that there is a large low luminosity galactic mass accumulation around the bulge. In our case of interest the mass estimate is taken to be 0.76×10^{42} kg at the distance of 16 kpc to match the rotational speed which peaks at ≈ 320 km/s. The mass estimate could be on the low side as we move towards 200 kpc due to mass distribution at larger distances between 16 kpc to 200 kpc. With this approximation we see in Fig. 1a that the rotational speeds from Eq.(3.1) matches the observations extremely well upto 100kpc. We also note that the Newtonian theory is quite sufficient up to 200 kpc and the eDM becomes dominant at much larger distances. In Fig. 1b, with the eDM term a mass estimate below 2.0×10^{42} kg (eg. 1.4×10^{42}kg) is enough to account for the observed rotational speed at 200 kpc. We also expect another eDM induced flattening of rotational curve from 300 kpc onward toward an upper bound value of 97 km/s given by a current Milky Way mass estimate of 3×10^{42} kg upto 2 Mpc which is the cut-off distance given in Eq.(3.10). We have neglected the $\ddot{a}/a$ term for simplicity. We see that the eDM can produce a flatten rotational curve at large distances, but the famous first flatten curve at $9 \sim 30$ kpc is only caused indirectly by the the eDM modification to the Newton's law. (We also calculate the Mercury perihelion advance rate due to this eDM resulting in $\sim O(10^{-3})$ arcsec per century, which is much less than the 41 arcsec per century due to the relativistic correction term. Therefore the eDM effect will be insignifcant in solar system gravity considerations.) From Fig. 1b if there is no cut-off distance, the thick solid line due to Eq.(3.3) could increase, crossing the MOND estimate at

$v^4 = GMa_0$, towards the value of $v^4 = 3GMa_0$ in Eq.(3.4) at the Hubble radius. However, the observed cut-off sizes of spiral galaxy are usually less than 10^{23} m [11], which constrain the rotational curve to stay closed to the MOND approximation, ensuring MOND's success in galactic considerations.

The eDM dynamical mass and density in the Milky Way and galaxy clusters:

To estimate the dynamical mass of this eDM within a cutoff radius R_{cutoff}, we imagine that the eDM is some real matter and have a matter density around the centre of Mass of the galaxy. Putting the dark matter term in Eq. (2.10) on the same footing of baryonic matter, we have the total dynamical mass of eDM within a spherical shell as a function of r

$$M_{eDM} = H\sqrt{\frac{M_b r^3}{2G}};\ \ \rho_{eDM} = \frac{3H}{4\pi}\sqrt{\frac{M_b}{2Gr^3}} = \sqrt{\frac{3H^2}{8\pi G}}\sqrt{\rho_b}. \tag{3.19}$$

While the total eDM dynamical mass will increase until it reaches the cut-off radius, we note that eDM density will drop off as $1/\sqrt{r^3}$. Using the cutoff radius Eq.(3.7) we obtain a simple relation

$$\frac{M_{eDM}}{M_b} = \frac{2}{(1-8q)^{1/2}-1} \tag{3.20}$$

for q_0 range of value in Eq. (3.10) we find

$$M_{eDM} \approx 2.0 \sim 2.15 \times M_b. \tag{3.21}$$

The total mass of the Milky Way to luminous mass ratio is $3 \sim 3.15$. If the galaxy is in a sufficiently isolated region the matter density of the eDM in this region is then given by

$$\frac{\rho_{eDM}}{\rho_b} = \frac{2}{(1-8q)^{1/2}-1}. \tag{3.22}$$

From [5] and [14-15] for X-ray groups and clusters of galaxies, the total mass to observable mass ratio can reach ≥ 7 which suggests the necessity of dark matter particles. However in the dark energy dominant epoch, from either best fit estimate [16] or a model with a cosmological constant, the deceleration parameter $q(z)$ will go to zero as $z \to z_T \approx 0.5$, where z_T is the transition point after which the dark energy begins its dominance.
For $q \approx -0.05 \sim -0.1$, the total mass will increase to $6.85M_b \sim 11.92M_b$.

However, precise determination of $q(z)$ value around z_T is not easy, for example for $z = 0.3$ the best fit models of [16] will give $q = -0.1 \sim -0.205$ with large error bars. We also note that in X-ray cluster calculations the dynamical mass estimate $M_N(r)$ for an isotropic isothermal sphere in hydrostatic equilibrium in [14] is proportional to the gas density ρ and temperature T at distance r from the centre of sphere:

$$M_N(r) \propto [\frac{d\ln(\rho)}{d\ln(r)} + \frac{d\ln(T)}{dr}]_r \tag{3.23}$$

From our analysis of the spiral galaxy above, whenever there is high enough mass density concentration in the cluster, the eDM potential through accretions will increase the gas density distribution around a Newtonian dominant regime at some distance r_{eq}, this should also reduce the value of $M_N(r)$ estimate. It is worth noting that for Milky Way size galaxy the eDM becomes significant from 0.1Mpc. For a cluster of size 10Mpc, there could be more dynamical mass distribution in the central region of the cluster coming from the eDM around individual smaller galaxies, in contrast to the simple halo picture of a spiral galaxy. Although we observe that Eq.(3.20,3.21,3.22) will fail for small q, in this case it simply means the cluster has no well defined cut-off.

4 Density perturbation evolution

At times before recombination, it is generally assumed that the overdense regions from inflation within the horizon will evolve into clusters of galactic objects. Dark collisionless particles will move into the centre of the perturbation both logarthmically in time during radiation epoch, and $\sim t^{2/3}$ during matter dominant epoch. The clumping of dark matter particles enhances the gravitational potential to assist baryonic matters to fall in faster after recombination. However, the eDM density in the matter dominant epoch is just a multiplicative factor of the uniform mass density and does not gravitate into the centre of perturbation before the recombination. To estimate the growth rate of small density perturbation in the matter dominant epoch under the influence of eDM, we note that the standard perturbation δ evolution equation is given by

$$\ddot{\delta} + 2H\dot{\delta} = 4\pi G\delta\rho \tag{4.1}$$

here the density perturbation δ is given by

$$\delta = \frac{\bar{\rho} - \rho}{\rho} \tag{4.2}$$

where $\bar{\rho}$ is the energy density of the overdense region of radius R, and ρ is the the background matter density. We use the standard derivations in [17] for the matter density of Eq. (3.1) the equation of motion for a point on the surface R is now

$$\frac{\ddot{R}}{R} = -\frac{4\pi}{3} G\rho(1 + \delta + \delta^{1/2}) \tag{4.3}$$

from Eq. (3.22) now the $\delta^{1/2}\rho$ term is the eDM density so that when $\delta = 0$ we recover the FRW solution. Here the total mass effective M within radius R is

$$M = (1 + \delta + \delta^{1/2})\rho(\frac{4\pi}{3} R^3) \tag{4.4}$$

Here although the eDM is not baryonic and does not participate in the CMB temperature fluctuations, it directly affects the fluctuation growth of the baryonic density. We consider the case that the total mass (baryonic matter plus eDM) within the overdense region radius R remains constant over time whilst $R(t) = a(t)(1 + \delta + \delta^{1/2})^{-1/3}$ grows as background density reduces. We should have $\delta + \delta^{1/2}$ in place of δ in Eq. (4.1). Without the eDM density $\delta^{1/2}\rho$, fluctuations grows most in the matter dominant epoch where $H = 2/(3t)$, and Eq. (4.1) becomes

$$\ddot{\delta} + \frac{4}{3t}\dot{\delta} - \frac{2}{3t^2}\delta = 0. \tag{4.5}$$

In a flat, matter-only universe where $a(t) \sim t^{2/3}$, the density pertubations will grow at the rate, given $\mid \delta \mid \ll 1$

$$\delta \propto t^{2/3} \propto a(t); \;\; a(t) \propto \frac{1}{1+z} \tag{4.6}$$

which leads to a growth $\delta \propto 10^3$ that is much less than the required total fluctuations growth of $\delta \geq 10^5$. As the eDM density is far larger than the matter density in Eq.(4.1), as an approximation we can replace δ by $\delta^{1/2}$ in Eq.(4.1) and Eq.(4.5) and obtain a new growth rate for δ as $\delta \propto t^{4/3} \propto a(t)^2$ which produces a growth rate of $\delta \propto 10^6$ since recombination. After recombination the baryonic density perturbation driven by the eDM will grow much faster than without the eDM, this could explain the large scale structure growth and Early Ionisation. The attractive background acceleration due to a large positive deceleration parameter q will also contribute. We also notice that after recombination the high eDM density should induce strongly the baryonic matter from the edge to fall towards the centre of the

overdense region very rapidly and thus will suppress the Baryon Acoustic Oscillations (BAO). This suppression is a major problem for MOND.

We note from [18] that within the MOND approximation the first and second acoustic peaks in WMAP can be obtained with Baryonic matter alone. The lifting of the third compression peak is regarded as a major evidence for CDM since here baryonic matter alone is not enough to lift the odd peaks and MOND has no effect in the high acceleration region before recombination. The equation for the evolution of a single k-mode of the perturbation in density, δ, for fluctuation with small fractional amplitude is given by

$$\ddot{\delta}_k + 2H\dot{\delta}_k + \delta c_s^2 k^2 = 4\pi G \delta_k \rho \tag{4.7}$$

where c_s is the sound speed given by

$$c_2^2 = \frac{c^2}{3(1+\tilde{R})}, \quad \tilde{R} = \frac{3\rho_b}{4\rho_\gamma} \tag{4.8}$$

where ρ_γ is the photon density [19-20]. From the unperturbed Poisson equation, one replaces the term $-4\pi G\rho\delta$ by $k^2\phi_k$. The effect of the solution of Eq. (4.7) on the temperature fluctuations is

$$\frac{\Delta T}{T} = \phi_k + \frac{1}{3}\delta_k = \frac{(1+3\tilde{R})}{3}\phi_k cos(c_s k t) - \tilde{R}\phi_k \tag{4.9}$$

In the matter dominant epoch, from Eq. (3.19) we have

$$\rho_{eDM} = \delta^{1/2}\sqrt{\rho_b}\sqrt{\rho_b} = \frac{1}{\delta^{1/2}}(\delta\rho_b). \tag{4.10}$$

The matter potential ϕ_k is now dominated by the eDM term. Since the radiation density is not enhanced and baryons are still strongly coupled to photons. We can assume that the eDM enhancement only affects the gravitational potential while the photon-baryon fluid pertubation δ continues to drive the oscillations. Similar analysis in Eq. (4.7-4.9) suggests that the first and second peak should behave similarly to that of CDM and MOND. For higher peaks which enter the horizon earlier, we need to involve radiation. In the radiation dominant epoch, we have no immediate guidance from previous sections on how the eDM will behave. From Eq. (2.4,2.6) in the simplest case that non-gravitating radiation density is not enhanced by the background density, we have

$$\rho_{eDM} = \delta^{1/2}\sqrt{\rho_b \cdot \rho_\gamma}. \tag{4.11}$$

which provides a larger potential than that of $\delta^{1/2}\rho_b$ in the matter dominant epoch, and the matter-radiation ratio is given by

$$\frac{\rho_m}{\rho_\gamma} = \frac{1}{\delta^{1/2}}\sqrt{\rho_b/\rho_\gamma}. \tag{4.12}$$

which could provide a dark matter density $\Omega_m h^2$ that is larger than $\Omega_b h^2$ at the recombination. In the radiation dominant CDM scenario, the strong radiation density leads to a decaying and oscillating potential in phase with the acoustic oscillations [19,20]. With the eDM this same "radiation driving" mechanism for CDM should lift the higher peaks. Alternatively we could have radiation density enhancement by an expanding background so that

$$\rho_{eDM} = \sqrt{\frac{3H^2}{8\pi G}}(\sqrt{\delta\rho_b} + \sqrt{\delta\rho_\gamma}) \tag{4.13}$$

In the radiation dominant epoch, the eDM becomes

$$\rho_{eDM} = \delta^{1/2}(\rho_\gamma + \sqrt{\rho_b . \rho_\gamma}). \tag{4.14}$$

Here the radiation density is also enhanced by background density, we expect that the enhanced radiation density will not gravitate but will provide enhanced pressure when compressed. Both radiation and matter density are now dominated by the eDM term in Eq. (4.14). The matter-radiation ratio becomes $\sqrt{\rho_b/\rho_\gamma}$. In Eq. (4.7) effectively we can replace the δ term by $\delta^{1/2}$. Similar argument on lifting of higher peaks goes through as in the no-enhancement case. So it is clear that the eDM can lead to the lifting the higher acoustic peaks, although more work is needed to understand the behaviour of relativistic matter in this metric. Empirically, the no enhancement scenario appears to be favoured by observations such as the Bullet cluster.

5 Summary

The issues around the nature of dark matter remains unresolved. With no modification of Einstein Gravity, we find that in a Single-metric approach for a spherical symmetric region with central mass concentration in the FRW background to possess an eDM term in the slow speed limit of its particle equation of motion. This solution has no free parameter and the eDM term has a built-in dependence on the Hubble parameter. This eDM density can vary from being a large factor of an uniform mass density in an overdense

region in the matter dominant epoch to becoming a massive halo density in the dark energy dominant epoch. We show how this new eDM term can account for some observations which motivate the need for dark matter in different epochs and could provide answers for other difficulties that is not fully explained by the MOND approximation.

Acknowledgement: C.C.W thanks Prof. Ron. Hui and the Electrical and Electronic Engineering Department at the University of Hong Kong for the support of this work.

References

1. G. A, Baker Jr., "Effects on the structure of the universe of an accelerating expansion" arXiv:astro-ph/0112320;
2. C. Dyer and C. Oliwa, "The "Swiss cheese" cosmological model has no extrinsic curvature discontinuity: A comment on the paper by G.A. Baker, Jr (astro-ph/0003152), arXiv:astro-ph/0004090v1.
3. P.A.R. Ade, N. Aghanim, C. Armitage-Caplan; et al. (Planck Collaboration) (22 March 2013) "Planck 2013 results. I. Overview of products and scientific results- Table 9" Astronomy and Astrophysics (submitted) 1303:5062. arXiv:1303.5062.
4. C. Moni Bidin, G. Carraro, R.A. Méndez, R. Smith, "Kinematical and chemical vertical structure of the Galactic thick disk II. A lack of dark matter in the solar neighborhood", arXiv:1204.3924, accepted for publication for the Astrophysical Journal.
5. A. Aguirre "Alternatives to Dark matter(?)" arXiv:astro-ph/0310572v2; "Dark matter in Cosmology" in "Dark matter in the Universe: Jerusalem Winter School for Theoretical Physics 1986-1987" pp.1-17.
6. T. Clifton, P.G. Ferreira, A. Padilla, C. Skordia, "Modified Gravity and Cosmology" arXiv:1106.2476v3, Physics Reports 513, 1 (2012), 1-189.
7. C. Skordia, "The Tensor-Vector-Scalar theories theory and its cosmology", arXiv:astro-ph/0903.3602v1.
8. S. McGaugh, "A tale of two paradigms: the mutual incommensurability of ΛCDM and MOND. arXiv:1404.7525, Canadian Journal of Physics 93,250 (2015); B. Famaey, S. McGaugh, "Challenges for Lambda-CDM and MOND", arXiv: 1301.0623, Proceedings of the Meeting of the International Association for Relativistic Dynamics, IARD 2012, Florence.
9. Philip D. Mannheim, "Alternatives to Dark Matter and Dark Energy", arXiv:astro-ph/0505266v2, Prog. Part. Nuvl. Phys. 56 (2006) 340-445.

10. B. Gumjudpai, "Quintessential power-law cosmology: dark energy equation of state", arXiv:1307.4552v1, Mod. Phys. Lett. A, Vol. 28, No. 29 (2013) 1350122.
11. H. Hoekstra, H.Yee, M. Gladders, Proceedings for "Where's the matter? Tracing dark and and bright matter with the new generation of large scale surveys", Marseille, 2001, arxiv:astro-ph/0109514.
12. J. Daboul, M. Nieto, "Exact, E=0, solutions for general power-law potentials. I Classical orbits". arXiv:hep-th/9408057, Phys. Rev. E52 (1955)4430.
13. P. Bhattacharjee, S. Chaudhury and S. Kundu, " Rotational Curve of Milky Way out to $\sim$ 200 kpc", arXiv:1310.2659v3, version accepted for publication in Apj.
14. R. Sanders, " Clusters of galaxies with Modified Newtonian dynamics", arXiv:astro-ph/0212293v1, Mon. Not. R. Astron. Soc., 000,000-000 (2002).
15. G. Angus, B. Famaey, D. Buote, "X-ray group and clsuter mass profiles in MOND: Unexplained mass in group scale", arXiv:0709.0108, accepted in MNRAS.
16 L. Xu, C. Zhang, B. Chang and H. Liu, "Reconstruction of deceleration parameter from recent cosmic observations", arXiv:astro-ph/0701519.
17. D. Erb,"University of Wisconsin Milwaukee, Astron401, lecture 36-37 ".
18. S. McGaugh, "Confrontation of MOND predictions with WMAP first year Data", arXiv:astro-ph/0312570, Astrophys. J. 611 (2004) 26-39.
19. W. Hu, N. Sugiyama, Astrophys. J 471(1996) 542.
20. W. Hu, S.Dodelson, Ann. Rev. Astron. Astrophys. 40:171-216, 2002, arXiv:astro-ph/0110414 .

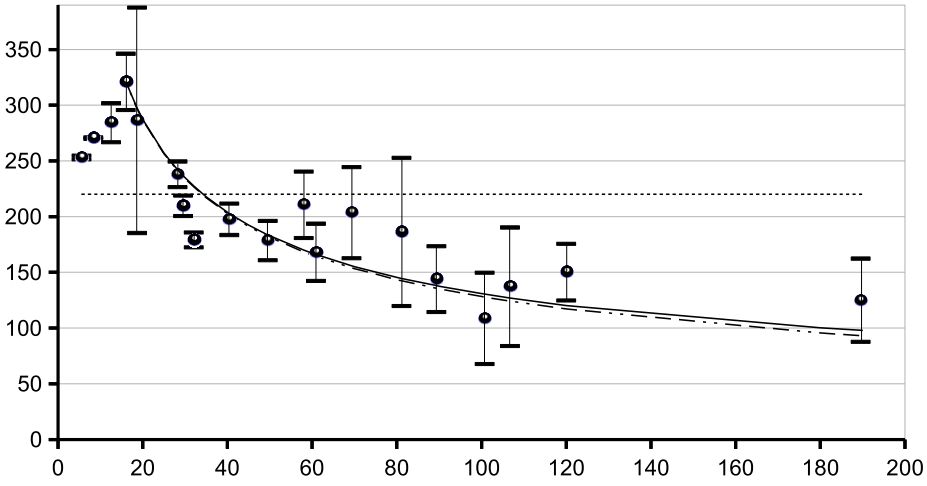

Figure 1a: Plot of the rotational speeds vs the distances from Milky Way centre, where the solid line is the results from Eq.(3.1) for mass at 0.76×10^{42} kg, the dashed line is the Newtonian speeds and the dots with error bars are the observational results from Ref.13 Table 2. The dotted line is a MOND estimate at $\upsilon = 220$ km/s.

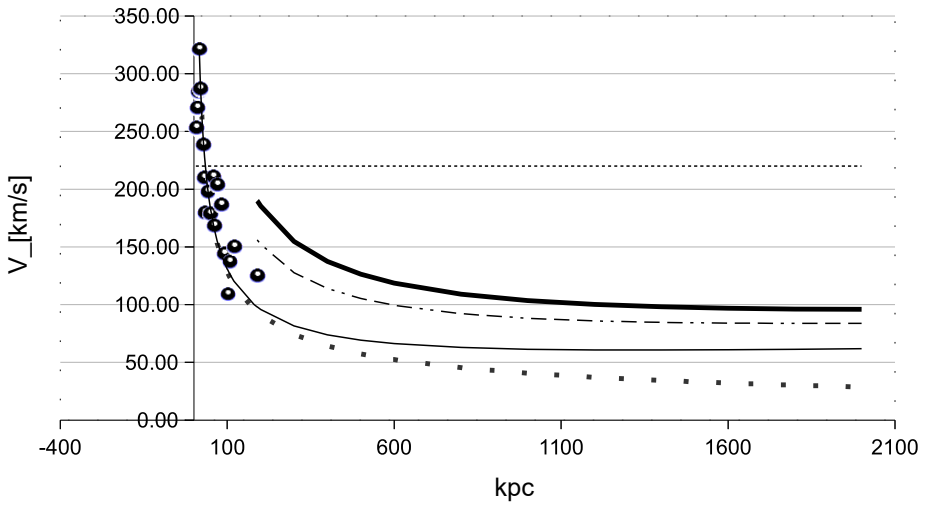

Figure 1b: Plot of the rotational speeds vs the distances from the Milky Way centre, where the thin solid line, the thin dashed line and thick solid line are the results from Eq. (3.1) for mass at 0.76×10^{42} kg and 2×10^{42} kg and 3×10^{42} kg respective-ly. The dots are the observational results from Ref.13 Table 2. The large dotted line is the Newtonian speeds for mass at 0.76×10^{42} kg and the fine dotted line is a MOND estimate at $\upsilon = 220$ km/s.